Sigma J Eng Nat Sci, Vol. 43, No. 6, pp. 2186–2197, December, 2025

Sigma Journal of Engineering and Natural Sciences
Web page info: https://sigma.yildiz.edu.tr
DOI: 10.14744/sigma.2025.1935

Research Article

Cosine Kumaraswamy family of distributions: Properties and applications to real-world datasets

Ibrahim ALI[1], Alhaji Modu ISA[1], Sule Omeiza BASHIRU[2,*], Arum Kingsley CHINEDU[3]

[1]Department of Mathematics and Computer Science, Borno State University, Maiduguri, 602104, Nigeria
[2]Department of Mathematics and Statistics, Confluence University of Science and Technology, Osara, Kogi State, 2344, Nigeria
[3]Department of Statistics, University of Nigeria, Nsukka, 900001, Nigeria

ARTICLE INFO

Article history
Received: 27 August 2024
Revised: 03 October 2024
Accepted: 31 October 2024

Keywords:
Cosine Family of Distributions, Order Statistics, Maximum Likelihood Estimation, Quantile Function, Lomax Distribution

ABSTRACT

This study presents the cosine Kumaraswamy family of distributions, a new family of probability distributions formed by combining the cosine and Kumaraswamy families. Several statistical properties of the family are derived, such as the quantile function, moments, moment-generating function, survival and hazard functions, and order statistics. The model parameters are estimated using the maximum likelihood method. A special case, called the cosine Kumaraswamy Lomax distribution, is discussed in detail, and its probability density and hazard functions are explored for different parameter values. To assess its usefulness, the cosine Kumaraswamy Lomax distribution is compared with other well-known models using three real datasets from the medical and engineering fields. The findings show that this distribution provides a better fit than the competing models, proving its flexibility and suitability for different types of data. Overall, the cosine Kumaraswamy family offers a useful addition to statistical modeling with strong practical applications.

Cite this article as: Ali I, Isa AM, Bashiru SO, Chinedu AK. Cosine Kumaraswamy family of distributions: Properties and applications to real-world datasets. Sigma J Eng Nat Sci 2025;43(6):2186–2197.

INTRODUCTION

The need for flexible probability distributions has become important in statistical research because they help describe different kinds of data more accurately and support reliable analysis in areas such as engineering, finance, and biological sciences. This interest has led to the creation of generalized families of distributions, known as generators, which extend traditional models by adding extra parameters. These added parameters allow the new distributions to handle complex data features like heavy tails and varying failure rates. The main goal of these developments is to create models that provide a better fit for various types of data. However, it is well known that no single distribution can describe all kinds of data, so researchers continue to design new probability distributions to meet this need.

In recent years, several new families of probability distributions have been developed to improve how data are modeled in different areas such as economics, engineering,

***Corresponding author.**
*E-mail address: bash0140@gmail.com

This paper was recommended for publication in revised form by Editor-in-Chief Ahmet Selim Dalkilic

biology, environmental studies, medicine, and finance. Well-known examples include the Kumaraswamy-G family [1], Weibull-G family [2], power Lindley-G family [3], weighted exponentiated-G family [4], sine Kumaraswamy-G family [5], sine Topp-Leone-G family [6], Topp-Leone odd exponential half logistic-G family [7], extended cosine generalized family [8], Sec-G family [9], logistic cotangent exponentiated generalized family [10], sine type II Topp-Leone family [11], cosine Topp-Leone family [12], secant Kumaraswamy family [13], and exponentiated cosine Topp-Leone family [14].

Building on this foundation, this study introduces a new family of probability distributions called the cosine Kumaraswamy family. It is formed by combining the Kumaraswamy and cosine families of distributions. This integration brings together the parameter-driven flexibility of the Kumaraswamy model with the trigonometric structure of the cosine model, resulting in a more versatile framework. The new family is better able to capture variations in skewness, kurtosis, and tail behavior than many existing models. The Lomax distribution emerges as a special case of this family and showed a better fit for some real datasets than the related submodels. The cosine Kumaraswamy family increases the applicability of classical distributions and serves as a flexible tool for modeling real-world data.

MATERIALS AND METHODS

The cumulative distribution function (cdf) and the probability density function (pdf) of the Kumaraswamy family of distributions (FOD) are expressed in equations (1) and (2) as follows:

$$R(x) = 1 - \left[1 - G(x)^{\theta}\right]^{\lambda} \tag{1}$$

$$r(x) = \lambda\theta g(x) G(x)^{\theta-1}\left[1 - G(x)^{\theta}\right]^{\lambda-1} \tag{2}$$

where $\lambda > 0$ and $\theta > 0$ are shape parameters, while $g(x)$ and $G(x)$ represent the pdf and cdf of a baseline distribution, respectively.

The cdf of the cosine FOD is given by:

$$F(x) = 1 - cos\left[\frac{\pi}{2}R(x)\right] \tag{3}$$

The corresponding pdf is:

$$f(x) = \frac{\pi}{2} r(x) sin\left[\frac{\pi}{2}R(x)\right] \tag{4}$$

By substituting equations (1) and (2) into equations (3) and (4), we get the cdf and pdf of the cosine Kumaraswamy (CK)-G FOD as follows:

$$F(x) = 1 - \cos\left\{\frac{\pi}{2}\left[1 - \left(1 - G(x)^{\theta}\right)^{\lambda}\right]\right\} \tag{5}$$

$$f(x)=\frac{\pi}{2}\lambda\theta g(x)G(x)^{\theta-1}\left[1-G(x)^{\theta}\right]^{\lambda-1}\sin\left\{\frac{\pi}{2}\left[1-\left(1-G(x)^{\theta}\right)^{\lambda}\right]\right\} \tag{6}$$

The survival function $S(x)$, hazard function $h(x)$, reverse hazard function $rh(x)$, and the cumulative hazard function $R(x)$ for the CK-G FOD are given in equations (7) to (10):

$$S(x) = cos\left\{\frac{\pi}{2}\left[1 - \left(1 - G(x)^{\theta}\right)^{\lambda}\right]\right\} \tag{7}$$

$$h(x)=\frac{\pi}{2}\lambda\theta g(x)G(x)^{\theta-1}\left[1-G(x)^{\theta}\right]^{\lambda-1}tan\left\{\frac{\pi}{2}\left[1-\left(1-G(x)^{\theta}\right)^{\lambda}\right]\right\} \tag{8}$$

$$rh(x)=\frac{\frac{\pi}{2}\lambda\theta g(x)G(x)^{\theta-1}\left[1-G(x)^{\theta}\right]^{\lambda-1}sin\left\{\frac{\pi}{2}\left[1-\left(1-G(x)^{\theta}\right)^{\lambda}\right]\right\}}{1-cos\left\{\frac{\pi}{2}\left[1-\left(1-G(x)^{\theta}\right)^{\lambda}\right]\right\}} \tag{9}$$

$$R(x) = -ln\left\{cos\left\{\frac{\pi}{2}\left[1 - \left(1 - G(x)^{\theta}\right)^{\lambda}\right]\right\}\right\} \tag{10}$$

Quantile Function

The quantile function of the CK-G FOD is given as:

$$\phi(u) = x = G^{-1}\left\{\left[1 - \left[1 - \frac{\cos^{-1}(1-u)}{\pi/2}\right]^{\frac{1}{\lambda}}\right]^{\frac{1}{\theta}}\right\} \tag{11}$$

Mixture Representation

The pdf and the cdf of the CK-G FOD can be expanded using power series expansion as follows:

Expanding the sine function in the pdf of the proposed family using a Taylor series gives:

$$sin\left\{\frac{\pi}{2}\left[1 - \left(1 - G(x)^{\theta}\right)^{\lambda}\right]\right\} = \sum_{i=1}^{\infty}\frac{(-1)^i}{(2i+1)!}\left(\frac{\pi}{2}\right)^{2i+1}\left[1 - \left(1 - G(x)^{\theta}\right)^{\lambda}\right]^{2i+1}$$

$$\left[1 - \left(1 - G(x)^{\theta}\right)^{\lambda}\right]^{2i+1} = \sum_{j=0}^{\infty}(-1)^j\binom{2i+1}{j}\left(1 - G(x)^{\theta}\right)^{\lambda j}$$

$$\left(1 - G(x)^{\theta}\right)^{\lambda j+\lambda-1} = \sum_{k=0}^{\infty}(-1)^k\binom{\lambda j+\lambda-1}{k}G(x)^{\theta k}$$

$$f(x) = \sum_{i,j,k=0}^{\infty}\frac{(-1)^{i+j+k}}{(2i+1)!}\frac{\pi^{2i+2}}{2^{2i+2}}\binom{2i+1}{j}\binom{\lambda j+\lambda-1}{k}\lambda\theta g(x)G(x)^{\theta k+\theta-1}$$

$$Let\ \Psi_{i,j,k} = \frac{(-1)^{i+j+k}}{(2i+1)!}\frac{\pi^{2i+2}}{2^{2i+2}}\binom{2i+1}{j}\binom{\lambda j+\lambda-1}{k}$$

Therefore,

$$f(x) = \sum_{i,j,k=0}^{\infty}\Psi_{i,j,k}\ \lambda\theta g(x)G(x)^{\theta(k+1)-1} \tag{12}$$

The cdf of the proposed family can also be expanded using power series expansion as follows:

$$cos\left\{\frac{\pi}{2}\left[1-\left(1-G(x)^{\theta}\right)^{\lambda}\right]\right\}=\sum_{l=0}^{\infty}\frac{(-1)^{l}}{(2l)!}\frac{\pi^{2l}}{2^{2l}}\left[1-\left(1-G(x)^{\theta}\right)^{\lambda}\right]^{2l}$$

$$\left[1-\left(1-G(x)^{\theta}\right)^{\lambda}\right]^{2l}=\sum_{n=0}^{\infty}(-1)^{n}\binom{2l}{n}\left(1-G(x)^{\theta}\right)^{\lambda n}$$

$$\left(1-G(x)^{\theta}\right)^{\lambda n}=\sum_{p=0}^{\infty}(-1)^{p}\binom{\lambda n}{p}G(x)^{\theta p}$$

$$F(x)=1-\sum_{l,n,p=0}^{\infty}\frac{(-1)^{l}}{(2l)!}\frac{\pi^{2l}}{2^{2l}}\binom{2l}{n}\binom{\lambda n}{p}G(x)^{\theta p}$$

$$\text{Let } \omega_{l,n,p}=\frac{(-1)^{l}}{(2l)!}\frac{\pi^{2l}}{2^{2l}}\binom{2l}{n}\binom{\lambda n}{p}$$

Therefore,

$$F(x)=1-\sum_{l,n,p=0}^{\infty}\omega_{l,n,p}\,G(x)^{\theta p} \tag{13}$$

Equations (12) and (13) represent the reduced forms of the new family.

MATHEMATICAL PROPERTIES

Moment

The moment of the CK-G FOD is derived as follows:

$$\mu_{r}'=E(x^{r})=\int_{-\infty}^{\infty}x^{r}f(x)dx$$

$$\mu_{r}'=\sum_{i,j,k=0}^{\infty}\Psi_{i,j,k}\,\lambda\theta\int_{0}^{\infty}x^{r}\;g(x)G(x)^{\theta(k+1)-1}dx$$

$$\text{Let } \phi=\int_{0}^{\infty}x^{r}\,g(x)G(x)^{\theta(k+1)-1}dx \tag{14}$$

$$\mu_{r}'=\sum_{i,j,k=0}^{\infty}\lambda\theta\,\Psi_{i,j,k}\,\phi$$

Moment Generating Function (MGF)

The MGF of the CK-G FOD is given by:

$$M_{x}(x)=E(e^{tx})=\int_{-\infty}^{\infty}e^{tx}f(x)dx$$

$$M_{x}(x)=\sum_{i,j,k=0}^{\infty}\Psi_{i,j,k}\,\lambda\theta\int_{0}^{\infty}e^{tx}\;g(x)G(x)^{\theta(k+1)-1}dx$$

$$\text{Let } \rho=\int_{0}^{\infty}e^{tx}\;g(x)G(x)^{\theta(k+1)-1}dx \tag{15}$$

$$M_{x}(x)=\sum_{i,j,k=0}^{\infty}\lambda\theta\Psi_{i,j,k}\rho$$

Order Statistics

Let x_1, x_2, ..., x_n be a random sample of size n with pdf f(x) and cdf F(x). The pdf of the order statistics is given by:

$$f_{n:m}(x)=\frac{f(x)}{B(n,m-n+1)}[F(x)]^{n-1}[1-F(x)]^{m-n}$$

For the CK-G FOD, the pdf of the order statistics is given by:

$$f_{n:m}(x)=\frac{\sum_{i,j,k=0}^{\infty}\Psi_{i,j,k}\;\lambda\theta g(x)G(x)^{\theta(k+1)-1}}{B(n,m-n+1)}\left[1-\sum_{i,p=0}^{\infty}\omega_{i,n,p}\,G(x)^{\theta p}\right]^{n-1}\left[\sum_{i,p=0}^{\infty}\omega_{i,n,p}G(x)^{\theta p}\right]^{m-n} \tag{16}$$

PARAMETER ESTIMATION

Maximum Likelihood Estimation

Let x_1, x_2, ..., x_n be an observed random sample of size n from the CK-G family, then the likelihood function can be expressed as:

$$\ell=\prod_{i=1}^{n}\left[\frac{\pi}{2}\lambda\theta g(x)G(x)^{\theta-1}\left[1-G(x)^{\theta}\right]^{\lambda-1}sin\left\{\frac{\pi}{2}\left[1-\left(1-G(x)^{\theta}\right)^{\lambda}\right]\right\}\right]$$

Taking the natural logarithm, the log-likelihood function simplifies to

$$\begin{aligned}\log\ell=\;&n\log\left(\frac{\pi}{2}\right)+n\log(\theta)\;+n\log(\lambda)+\sum_{i=1}^{n}\log g(x)\\&+(\theta-1)\sum_{i=1}^{n}\log g(x)+(\lambda-1)\sum_{i=1}^{n}log\left[1-G(x)^{\theta}\right]\\&+\sum_{i=1}^{n}\log sin\left\{\frac{\pi}{2}\left[1-\left(1-G(x)^{\theta}\right)^{\lambda}\right]\right\}\end{aligned} \tag{17}$$

Now, we determine the first-order conditions

$$\begin{aligned}\frac{\partial\ell}{\partial\theta}=&\frac{n}{\theta}+\sum_{i=1}^{n}\log G(x)+(\lambda-1)-\sum_{i=1}^{n}\frac{G(x)^{\theta}\log G(x)}{(1-G(x)^{\theta})}\\&-\sum_{i=1}^{n}\frac{\pi}{2}\lambda\left(1-G(x)^{\theta}\right)^{\lambda-1}\times G(x)^{\theta}\log G(x)\tan\left\{\frac{\pi}{2}\left[1-\left(1-G(x)^{\theta}\right)^{\lambda}\right]\right\}\end{aligned} \tag{18}$$

$$\begin{aligned}\frac{\partial\ell}{\partial\lambda}=&\frac{n}{\lambda}+\sum_{i=1}^{n}\log(1-G(x)^{\theta})\\&-\sum_{i=1}^{n}\frac{\pi}{2}\left(1-G(x)^{\theta}\right)^{\lambda}\log(1-G(x)^{\theta})\tan\left\{\frac{\pi}{2}\left[1-\left(1-G(x)^{\theta}\right)^{\lambda}\right]\right\}\end{aligned} \tag{19}$$

$$\begin{aligned}\frac{\partial\ell}{\partial\xi}=&\sum_{i=1}^{n}\frac{g'(x)}{g(x)}+(\theta-1)\sum_{i=1}^{n}\frac{g(x)}{G(x)}-\sum_{i=1}^{n}\frac{\theta g(x)G(x)^{\theta-1}}{(1-G(x)^{\theta})}\\&-\sum_{i=1}^{n}\frac{\pi}{2}\lambda\theta g(x)G(x)^{\theta-1}\left(1-G(x)^{\theta}\right)^{\lambda-1}\tan\left\{\frac{\pi}{2}\left[1-\left(1-G(x)^{\theta}\right)^{\lambda}\right]\right\}\end{aligned} \tag{20}$$

Since obtaining closed-form solutions for this system of equations is challenging, numerical solutions can be found using iterative methods.

SUB-MODEL

We introduce the Lomax distribution, as proposed by [15], as a specific case within the CK-G distribution family. The cdf and pdf of the Lomax distribution are provided in equations (21) and (22) below.

$$G(x) = 1 - \left(1 + \frac{x}{\beta}\right)^{-\alpha} \tag{21}$$

$$g(x) = \frac{\alpha}{\beta}\left(1 + \frac{x}{\beta}\right)^{-(\alpha+1)} \tag{22}$$

where, $\alpha > 0$ and $\beta > 0$ are the shape and scale parameters respectively

Cosine Kumaraswamy – Lomax (CKL) Distribution

By substituting equation (21) into equation (5), the cdf of the cosine Kumaraswamy Lomax (CKL) distribution is given by:

$$F(x) = 1 - cos\left\{\frac{\pi}{2}\left[1 - \left(1 - \left(1 - \left(1 + \frac{x}{\beta}\right)^{-\alpha}\right)^{\theta}\right)^{\lambda}\right]\right\} \tag{23}$$

And by substituting equations (21) and (22) into (6), we have the associated pdf given as:

$$f(x) = \frac{\pi}{2}\lambda\theta\left(\frac{\alpha}{\beta}\left(1 + \frac{x}{\beta}\right)^{-(\alpha+1)}\right)\left(1 - \left(1 + \frac{x}{\beta}\right)^{-\alpha}\right)^{\theta-1} \times\left[1 - \left(1 - \left(1 + \frac{x}{\beta}\right)^{-\alpha}\right)^{\theta}\right]^{\lambda-1} sin\left\{\frac{\pi}{2}\left[1 - \left(1 - \left(1 - \left(1 + \frac{x}{\beta}\right)^{-\alpha}\right)^{\theta}\right)^{\lambda}\right]\right\} \tag{24}$$

The pdf and cdf plots of the CKL distribution are shown in Figure 1.

Figure 1 illustrates that the CKL distribution's pdf is approximately symmetric, right-skewed, and unimodal. The cdf starts at zero and approaches one, confirming its validity as a probability distribution.

The functions $S(x)$, $h(x)$, $rh(x)$, $R(x)$ and the $\phi(u)$ of the CKL distribution are given in equations (25) to (29):

$$S(x) = cos\left\{\frac{\pi}{2}\left[1 - \left(1 - \left(1 - \left(1 + \frac{x}{\beta}\right)^{-\alpha}\right)^{\theta}\right)^{\lambda}\right]\right\} \tag{25}$$

$$h(x) = \theta\lambda\left[\frac{\alpha x}{\beta}\left(1 + \frac{x}{\beta}\right)^{-(\alpha+1)}\right]\left[1 - \left(1 + \frac{x}{\beta}\right)^{-\alpha}\right]^{\theta-1} \times\left[1 - \left(1 - \left(1 + \frac{x}{\beta}\right)^{-\alpha}\right)^{\theta}\right]^{\lambda-1} tan\left\{\frac{\pi}{2}\left[1 - \left(1 - \left(1 - \left(1 + \frac{x}{\beta}\right)^{-\alpha}\right)^{\theta}\right)^{\lambda}\right]\right\} \tag{26}$$

$$rh(x) = \frac{\theta\lambda\left[\frac{\alpha x}{\beta}\left(1 + \frac{x}{\beta}\right)^{-(\alpha+1)}\right]\left[1 - \left(1 + \frac{x}{\beta}\right)^{-\alpha}\right]^{\theta-1}\left[1 - \left(1 - \left(1 + \frac{x}{\beta}\right)^{-\alpha}\right)^{\theta}\right]^{\lambda-1} sin\left\{\frac{\pi}{2}\left[1 - \left(1 - \left(1 - \left(1 + \frac{x}{\beta}\right)^{-\alpha}\right)^{\theta}\right)^{\lambda}\right]\right\}}{1 - cos\left\{\frac{\pi}{2}\left[1 - \left(1 - \left(1 + \frac{x}{\beta}\right)^{-\alpha}\right)^{\theta}\right)^{\lambda}\right]\right\}} \tag{27}$$

$$R(x) = -ln\left[cos\left\{\frac{\pi}{2}\left[1 - \left(1 - \left(1 - \left(1 + \frac{x}{\beta}\right)^{-\alpha}\right)^{\theta}\right)^{\lambda}\right]\right\}\right] \tag{28}$$

$$\phi(u) = \beta\left\{1 - \left(1 - \left(1 - \left(1 - \frac{\cos^{-1}(1-u)}{\frac{\pi}{2}}\right)^{\frac{1}{\lambda}}\right)^{\frac{1}{\theta}}\right)^{-\frac{1}{\alpha}}\right\} \tag{29}$$

The survival and hazard function plots of the CKL distribution are shown in Figure 2.

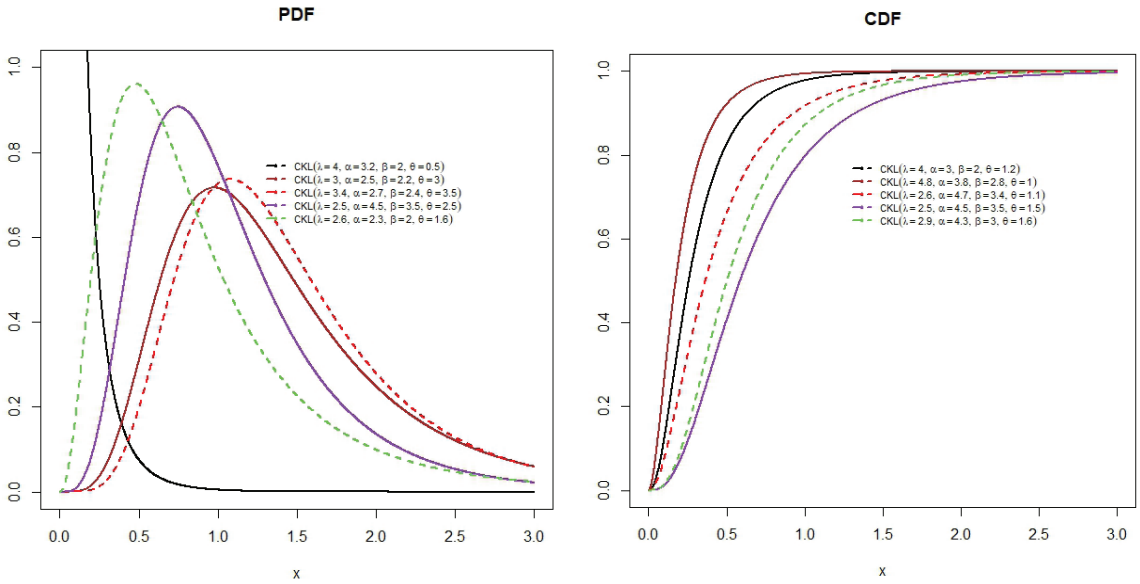

Figure 1. pdf and cdf plots of the CKL distribution.

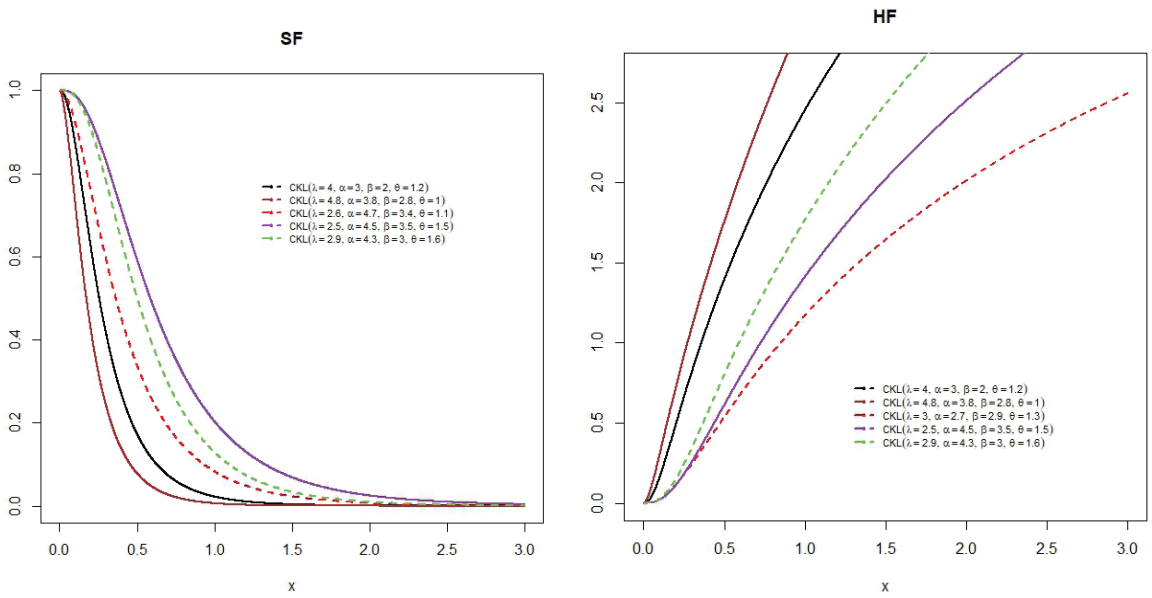

Figure 2. Survival function and Hazard function plots of the CKL distribution.

Figure 2 illustrates that the hazard function of the CKL distribution exhibits an increasing hazard rate, indicating that the risk of an event occurring rises over time. The survival function, on the other hand, decreases from 1 to 0, indicating a lower probability of survival with time.

APPLICATION

This section shows how useful the cosine Kumaraswamy Lomax (CKL) distribution is by applying it to three real datasets. The CKL model is compared with some well-known distributions, such as the Lomax (L) [16], Lehmann type II Lomax (LTIIL) [17], half-logistic Lomax (HLL) [18], and power Lomax (PL) [19] models. Model parameters are estimated using the maximum likelihood estimation (MLE) method. To compare the models, different goodness-of-fit criteria are used, such as the Akaike information criterion (I_A), Bayesian information criterion (I_B), corrected Akaike information criterion (I_{CA}), and Hannan–Quinn information criterion (I_{HQ}). The model with the smallest values of these measures gives the best fit to the data.

First Data

The first dataset, sourced from [20], consists of the number of million revolutions before failure recorded for 23 ball bearings during life tests. The data is as follows:

17.88, 28.92, 33.0, 41.52, 42.12, 45.6, 48.8, 51.84, 51.96, 54.12, 55.56, 67.8, 68.44, 68.88, 84.12, 93.12, 98.64, 105.12, 105.84, 105.84, 127.92, 128.04, 173.4.

Descriptive statistics for the first dataset are shown in Table 1, and the graphs are shown in Figure 3. The parameter estimates and goodness-of-fit results for the first dataset are shown in Table 2, with the estimated pdf, cdf, survival function, and P–P plots in Figure 4.

Table 1 shows the descriptive statistics for the first dataset, which indicate moderate positive skewness and a leptokurtic shape. These features are also shown in the plots in Figure 3. The kernel density plot supports the presence of positive skewness, while the TTT plot suggests an increasing failure rate. The box plot further shows that the dataset contains some outliers.

The goodness-of-fit measures in Table 2 indicate that our proposed CLK model outperforms the other distributions tested, as it has the lowest evaluation metric values. Figure 4 shows the fitted density, cdf, survival function (sf), and P–P plots of the CLK model for the dataset, indicating that the model fits the data very well.

Second Data

The second dataset, as discussed by [20], consists of failure times for 24 mechanical components. The observations are as follows:

Table 1. Descriptive statistics of the first data

Min	Mean	Median	Range	Skewness	Kurtosis	Max
17.88	73.85	67.80	155.52	0.7972	3.1410	173.4

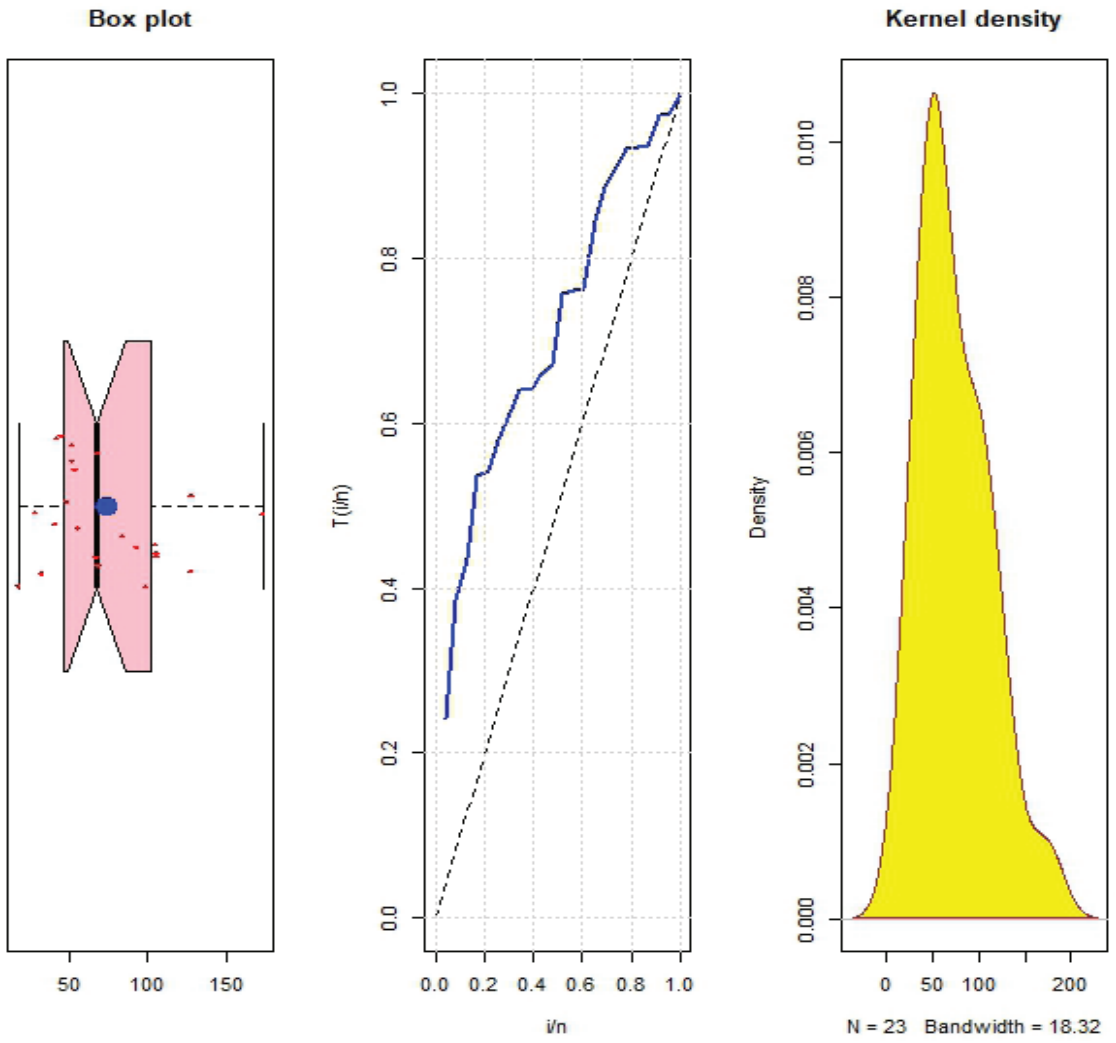

Figure 3. Visual representations of the first dataset.

Table 2. Goodness-of-fit measures for each distribution applied to the first dataset.

MODEL	MLE	-LL	I_A	I_B	I_{CA}	I_{HQ}
CKL	$\hat{\lambda} = 62.9734$ $\hat{\theta} = 268.109$ $\hat{\alpha} = 0.3772$ $\hat{\beta} = 0.00095$	113.9990	235.9980	240.5400	238.2202	237.1403
L	$\hat{\alpha} = 648816.1$ $\hat{\beta} = 47988211$	121.9459	247.8918	250.1628	248.4918	248.4629
LTIIL	$\hat{\gamma} = 0.0403$ $\hat{\alpha} = 13.5307$ $\hat{\lambda} = 12.6983$	136.9632	279.9263	283.3328	281.1895	280.783
HLL	$\hat{\alpha} = 1332.639$ $\hat{\beta} = 0.000015$	119.2122	242.4244	244.6954	243.0244	242.9956
PL	$\hat{\alpha} = 105.5535$ $\hat{\beta} = 0.55500$ $\hat{\lambda} = 800.9172$	134.881	275.762	279.1685	277.0251	276.6187

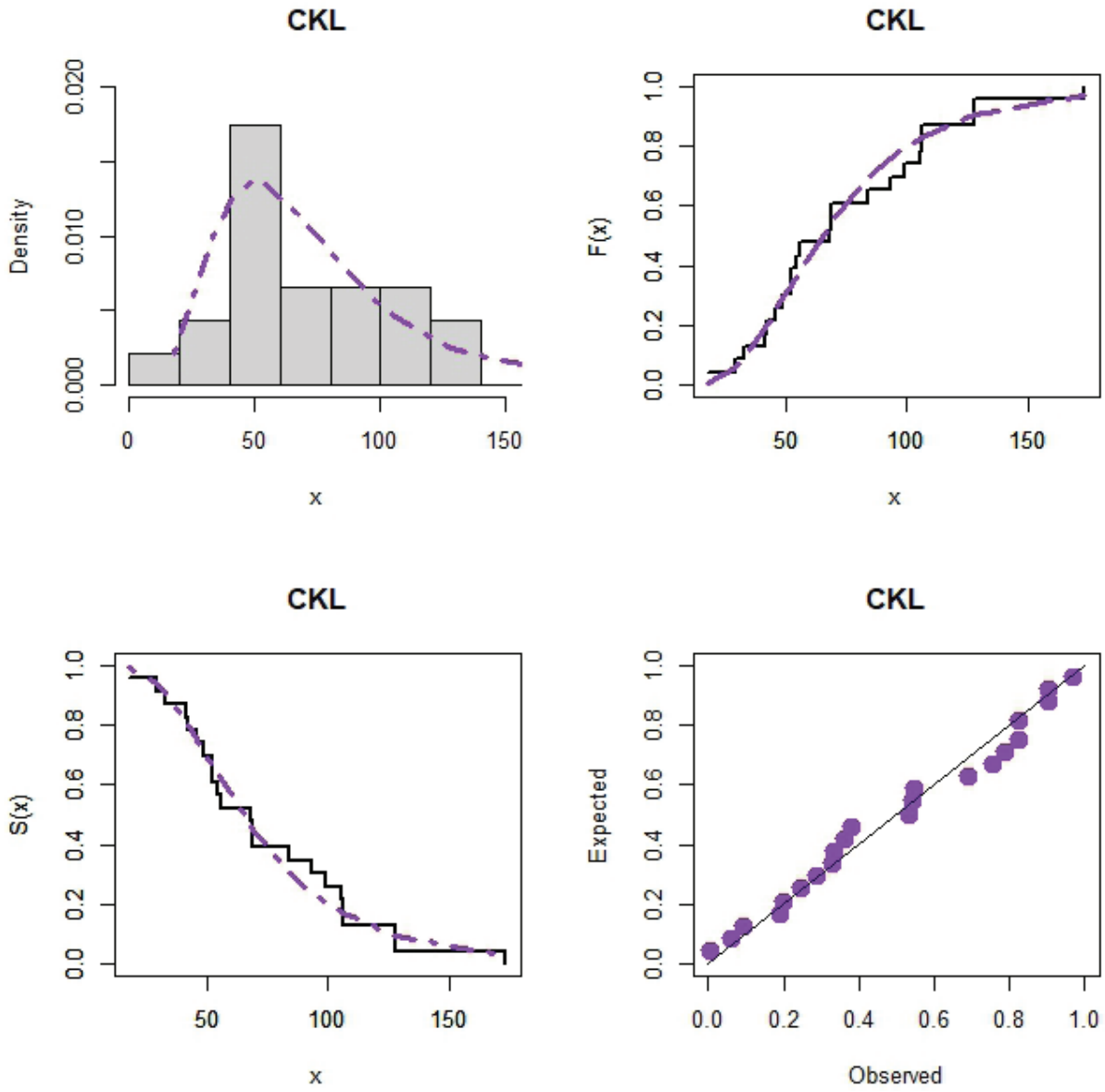

Figure 4. Fitted density, cdf, SF and PP plot of the CLK model to the first data.

30.94, 18.51, 16.62, 51.56, 22.85, 22.38, 19.08, 49.56, 17.12, 10.67, 25.43, 10.24, 27.47, 14.70, 14.10, 29.93, 27.98, 36.02, 19.40, 14.97, 22.57, 12.26, 18.14, 18.84

Descriptive statistics for the second dataset are shown in Table 3, and the graphs are shown in Figure 5. The parameter estimates and goodness-of-fit results for the second dataset are shown in Table 4, with the estimated pdf, cdf, survival functions, and P–P plots in Figure 6.

The descriptive statistics presented in Table 3 indicate that the dataset is highly positively skewed and leptokurtic. Figure 4 shows the presence of outliers in the box plot, while the TTT plot reveals an increasing failure rate. Additionally, the kernel density plot suggests that the dataset is right-skewed.

The goodness-of-fit measures in Table 4 indicate that our proposed CKL model outperforms the other distributions,

Table 3. Descriptive statistics of the second data

Min	Mean	Median	Range	Skewness	Kurtosis	Max
10.24	22.97	19.24	41.32	1.3454	4.3599	51.56

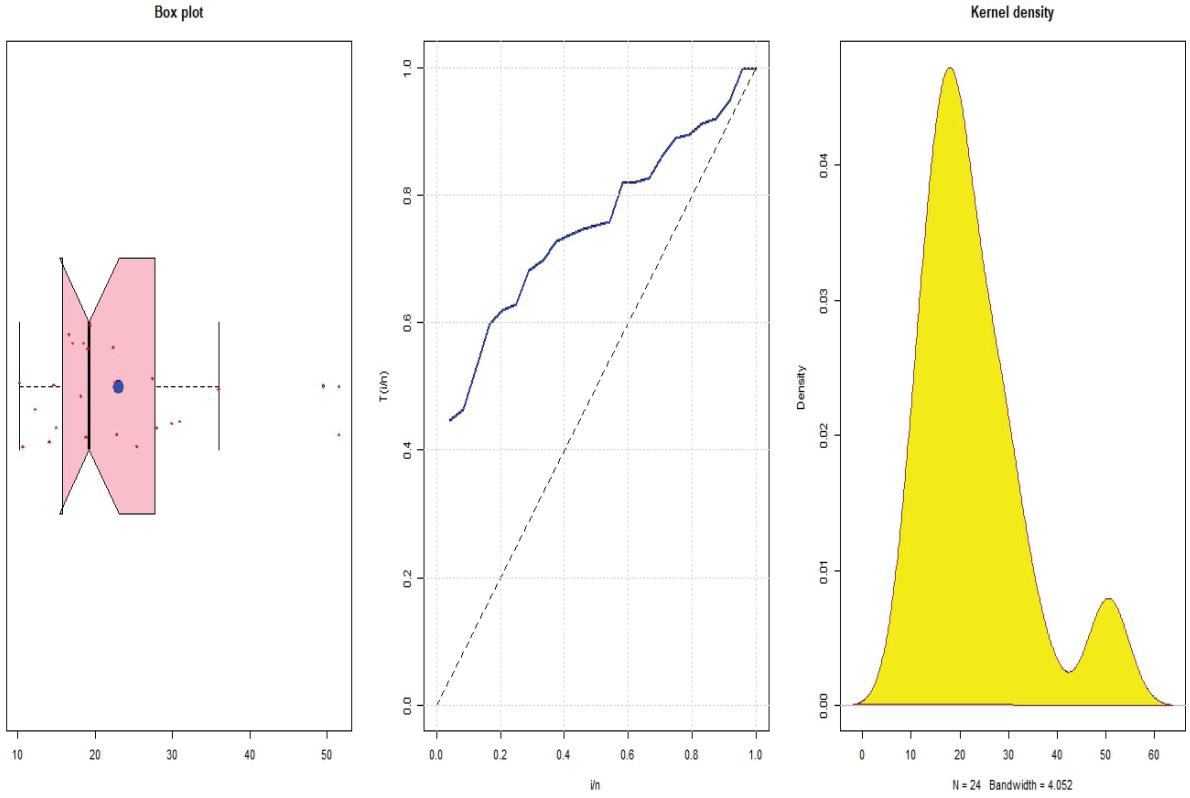

Figure 5. Visual representations of the second dataset.

Table 4. Goodness-of-fit measures for each distribution applied to the second dataset

MODEL	MLE	-LL	I_A	I_B	I_{CA}	I_{HQ}
CKL	$\hat{\lambda} = 0.221000$ $\hat{\theta} = 78.39050$ $\hat{\alpha} = 82262.37$ $\hat{\beta} = 179403.6$	85.5086	179.0174	183.7296	181.1226	180.2675
L	$\hat{\alpha} = 2061805$ $\hat{\beta} = 47372304$	99.2231	202.4463	204.8024	203.0177	203.0714
LTIIL	$\hat{\gamma} = 2.135900$ $\hat{\alpha} = 838177.7$ $\hat{\lambda} = 41118771$	99.2231	204.4463	207.9805	205.6463	205.3839
HLL	$\hat{\alpha} = 565.0091$ $\hat{\beta} = 0.00011$	95.9624	195.9249	198.281	196.4963	196.5499
PL	$\hat{\alpha} = 84.1146$ $\hat{\beta} = 1.29310$ $\hat{\alpha} = 4310.37$	94.9106	195.8214	199.3555	197.0214	196.7590

as evidenced by its lowest evaluation metric values. Figure 6 shows the fitted density, cdf, sf, and P–P plots of the CLK model for the dataset, indicating that the model fits the data very well.

Third Data

The third dataset, sourced from [21], includes the relief times (in minutes) for 20 patients treated with an analgesic.

"1.1, 1.4, 1.3, 1.7, 1.9, 1.8, 1.6, 2.2, 1.7, 2.7, 4.1, 1.8, 1.5, 1.2, 1.4, 3, 1.7, 2.3, 1.6, 2"

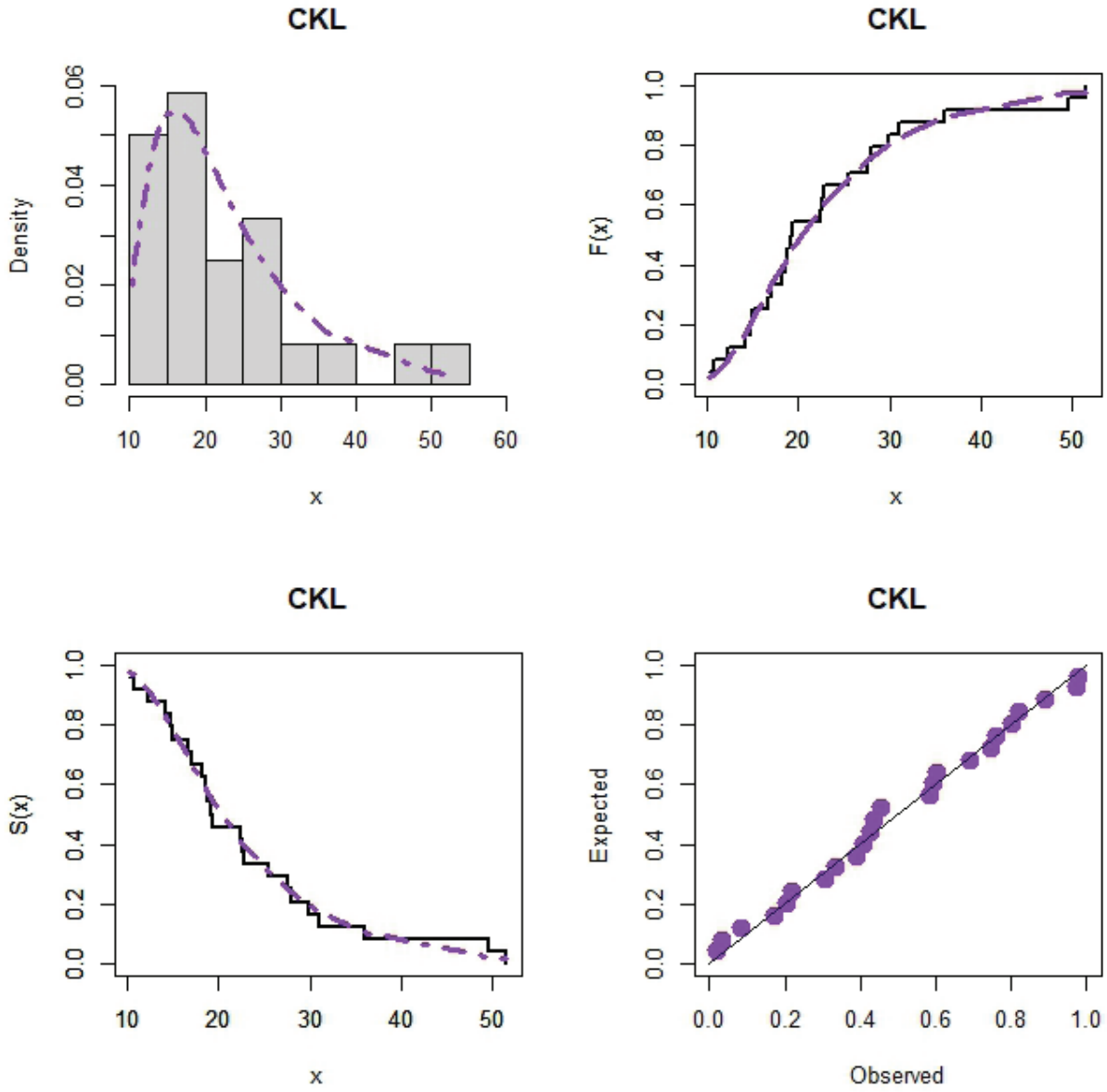

Figure 6. Fitted density, CDF, SF and PP plot of the CKL model to the second data.

Descriptive statistics for the third dataset are shown in Table 5, and the graphs are shown in Figure 7. The parameter estimates and goodness-of-fit results for the third dataset are shown in Table 6, with the estimated pdf, cdf, survival function, and P–P plots in Figure 8.

The descriptive statistics presented in Table 5 indicate that the dataset is highly positively skewed and leptokurtic. Figure 7 shows the presence of outliers in the box plot, while the TTT plot reveals an increasing failure rate. Additionally, the kernel density plot suggests that the dataset is right-skewed.

The goodness-of-fit results in Table 6 show that the proposed CKL model performs better than the other distributions, as it has the lowest values for the evaluation measures. Figure 8 shows the fitted density, cdf, sf, and P–P

Table 5. Descriptive statistics of the third data

Min	Mean	Median	Range	Skewness	Kurtosis	Max
1.1	1.9	1.7	3	1.7197	5.9241	4.1

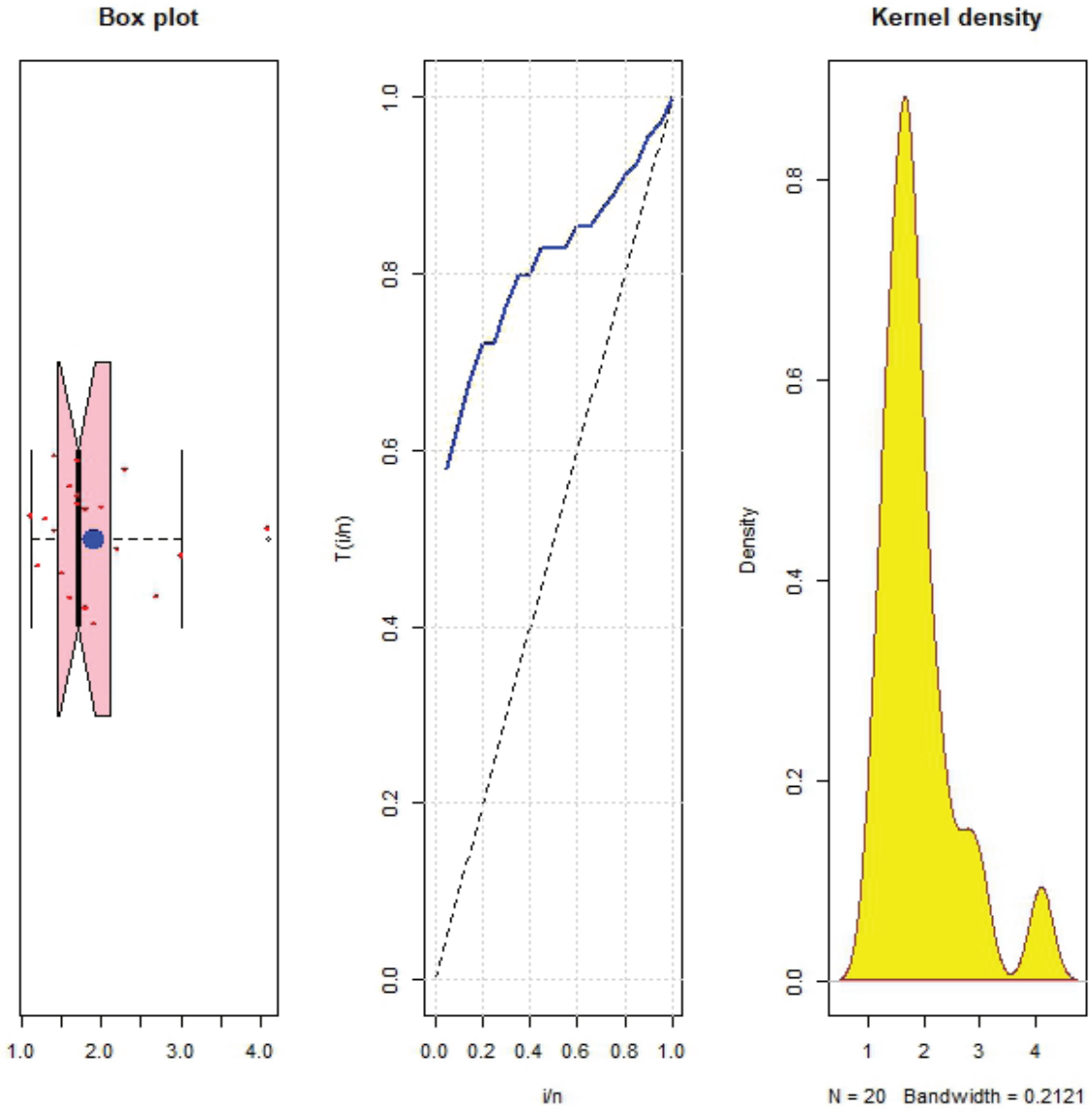

Figure 7. Visual representations of the third dataset.

Table 6. Goodness-of-fit measures for each distribution applied to the third dataset

MODEL	MLE	-LL	I_A	I_B	I_{CA}	I_{HQ}
CKL	$\hat{\lambda} = 5.79830$	15.9688	39.9376	43.9205	42.6043	40.7151
	$\hat{\theta} = 41.2967$					
	$\hat{\alpha} = 1.61060$					
	$\hat{\beta} = 0.28520$					
L	$\hat{\alpha} = 1929.1945$	32.83708	69.6742	71.6657	70.3800	70.0629
	$\hat{\beta} = 36673966$					
LTIIL	$\hat{\gamma} = 0.732000$	32.8371	71.6742	74.6614	73.1742	72.2573
	$\hat{\alpha} = 3357085$					
	$\hat{\lambda} = 4670060$					
HLL	$\hat{\alpha} = 3710.142$	29.6508	63.3016	65.2931	64.0075	63.6904
	$\hat{\beta} = 0.000200$					

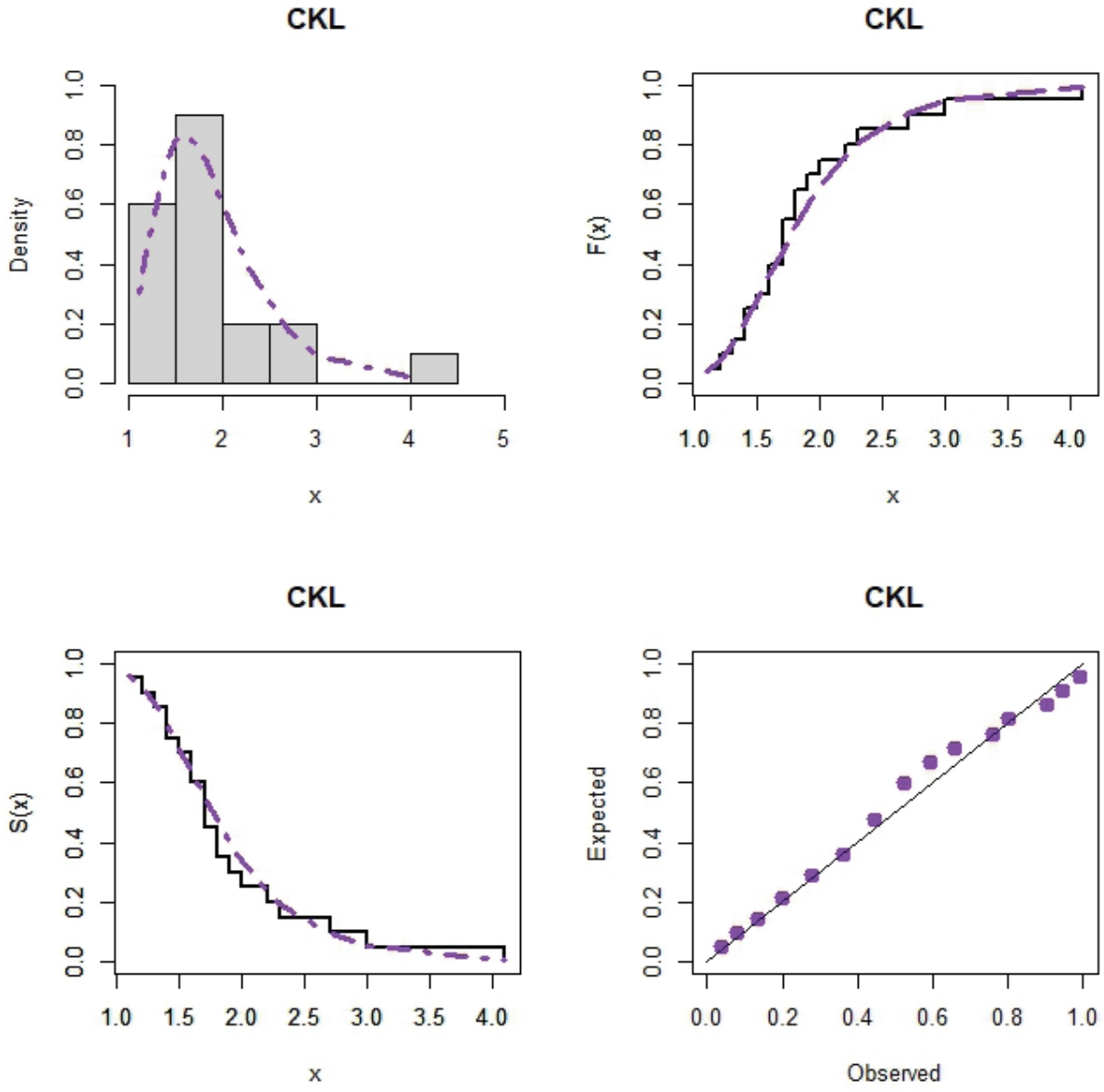

Figure 8. Fitted density, cdf, SF and PP plot of the CKL model to the third data.

plots of the CLK model for the dataset, indicating that the model fits the data very well.

RESULTS AND DISCUSSION

The cosine Kumaraswamy Lomax (CKL) distribution was applied to three real datasets from engineering and medical studies. The findings show that the CKL model is flexible and can handle different types of data. In all three cases, the CKL model performed better than the Lomax, Lehmann type II Lomax, half-logistic Lomax, and power Lomax models.

The lower I_A, I_B, I_{CA}, and I_{HQ} values show that the CKL model fits the data well. Results from the analysis of the two data indicate that the CKL model can be used in both engineering and medical studies. In engineering, it can be used to describe how long components last, helping improve maintenance and design. In medicine, it can be used to study relief times and support treatment choices.

CONCLUSION

This study introduced a new FOD called the cosine Kumaraswamy FOD, created by combining the Kumaraswamy and cosine families. The main properties of the family, such as the quantile function, moments, and order statistics, were derived.

A submodel of this family, the cosine Kumaraswamy Lomax (CKL) distribution, was proposed. Its performance was tested with three real datasets from engineering and medical fields and compared with other known models. The CKL model gave the best fit in all cases, showing that it can handle different types of data well.

The CKL distribution adds a useful tool to statistical modeling. Future work can build on this family to create new submodels with broader use and better performance in various areas.

REFERENCES

[1] Cordeiro GM, De Castro M. A new family of generalized distributions. J Stat Comput Simul 2011;81:883–898. [CrossRef]

[2] Bourguignon M, Silva RB, Cordeiro GM. The Weibull-G family of probability distributions. J Data Sci. 2014;12:53–68. [CrossRef]

[3] Hassan AS, Nassr SG. Power Lindley-G family of distributions. Ann Data Sci 2019;6:189–210. [CrossRef]

[4] Ahmad Z, Elgarhy M, Hamedani GG. The weighted exponentiated family of distributions: properties, applications and characterizations. J Iranian Stat Soc 2019;19:209–228. [CrossRef]

[5] Chesneau C, Jamal F. The sine Kumaraswamy-G family of distributions. J Math Ext 2020;15:1–26.

[6] Al-Babtain AA, Elbatal I, Chesneau C, Elgarhy M. Sine Topp-Leone-G family of distributions: theory and applications. Open Phys 2020;18:574–593. [CrossRef]

[7] Chipepa F, Oluyede B. The Topp-Leone odd exponential half logistic-G family of distributions: model, properties and applications. Pak J Stat 2021;37:253–277. [CrossRef]

[8] Mahmood Z, Jawa TM, Sayed-Ahmed N, Khalil EM, Muse AH, Tolba AH. An extended cosine generalized family of distributions for reliability modeling: characteristics and applications with simulation study. Math Prob Eng 2022;2022:3634698. [CrossRef]

[9] Souza L, de Oliveira WR, de Brito CCR, Chesneau C, Fernandes R, Ferreira TA. Sec-G class of distributions: properties and applications. Symmetry. 2022;14:299. [CrossRef]

[10] Tashkandy YA, Nagy M, Akbar M, Mahmood Z, Gemeay AM, Hossain MM, et al. The exponentiated cotangent generalized distributions: characteristics and applications to chemotherapy treatment data. IEEE Access 2023;11:35697–35709. [CrossRef]

[11] Isa AM, Doguwa SI, Alhaji BB, Dikko HG. Sine Type II Topp-Leone G family of probability distribution: mathematical properties and application. Arid Zone J Basic Appl Res 2023;2:124–138. [CrossRef]

[12] Nanga S, Nasiru S, Dioggban J. Cosine Topp-Leone family of distributions: properties and regression. Res Math 2023;10:2208935. [CrossRef]

[13] Nanga S, Sayibu SB, Angbing ID, Alhassan M, Benson AM, Abubakari AG, et al. Secant Kumaraswamy family of distributions: properties, regression model, and applications. Comput Math Methods 2024;2024:8925329. [CrossRef]

[14] Osi AA, Doguwa SI, Abubakar Y, Zakari Y, Abubakar U. Development of exponentiated cosine Topp-Leone generalized family of distributions and its applications to lifetime data. UMYU Scientifica 2024;3:157–167. [CrossRef]

[15] Souza L. New trigonometric classes of probabilistic distributions [master thesis]. State of Pernambuco, Brasil; 2015.

[16] Lomax KS. Business failures: another example of the analysis of failure data. J Am Stat Assoc 1954;49:847–852. [CrossRef]

[17] Isa AM, Kaigama A, Akeem AA, Sule OB. Lehman Type II Lomax distribution: properties and application to real data set. Commun Phys Sci 2023;9:63–72.

[18] Anwar M, Zahoor J. The half-logistic Lomax distribution for lifetime modeling. J Probab Stat 2018;2018:3152807. [CrossRef]

[19] Rady EHA, Hassanein WA, Elhaddad TA. The power Lomax distribution with an application to bladder cancer data. SpringerPlus 2016;5:1838. [CrossRef]

[20] Arshad MZ, Iqbal MZ, Al Mutairi A. A comprehensive review of datasets for statistical research in probability and quality control. J Math Comput Sci 2021;11:3663–3728.

[21] Bashiru SO. A study on the properties of a new exponentiated extended inverse exponential distribution with applications. Reliab Theory Appl 2023;3:59–72.